Contribution from the Lehrstuhl für Anorganische Chemie I, Ruhr-Universität, D-4630 Bochum, FRG, and Anorganisch-Chemisches Institut der Universität, D-6900 Heidelberg, FRG

(μ-Hydroxo)bis(μ-carboxylato)diruthenium and (μ-Oxo)bis(μ-carboxylato)diruthenium Complexes Containing Weak Intramolecular Ru···Ru Interactions

Peter Neubold,[1a] Karl Wieghardt,*[,1a] Bernhard Nuber,[1b] and Johannes Weiss[1b]

Received July 22, 1988

The hydrolysis reaction of $[LRuCl_3]\cdot H_2O$ (L represents 1,4,7-trimethyl-1,4,7-triazacyclononane, $C_9H_{21}N_3$) in aqueous solution (pH $\approx$ 7) containing a variety of carboxylic acids yields purple, diamagnetic (μ-oxo)bis(μ-carboxylato)diruthenium(III) dications where each ruthenium is capped by a tridentate cyclic amine L. The crystal structure of $[L_2Ru^{III}_2(\mu\text{-}O)(\mu\text{-}CH_3CO_2)_2](PF_6)_2\cdot 0.5H_2O$ has been determined by X-ray crystallography. Crystal data: orthorhombic; *Ibca* (D^{27}_{2h}, No. 73); a = 13.631 (4), b = 14.992 (8), c = 35.465 (8) Å; V = 7247.5 Å^3; ρ_{calcd} = 1.79 g/cm^3; Z = 8. Two pseudooctahedral Ru^{III} centers are connected by an oxo and two symmetrical acetato bridges (Ru···Ru = 3.258 (1) Å). In strongly acidic media the μ-oxo bridge is protonated (pK_a = 1.9, 25 °C), affording green $[L_2Ru_2(\mu\text{-}OH)(\mu\text{-}CH_3CO_2)_2](PF_6)_3$. The two Ru^{III} centers are strongly intramolecularly antiferromagnetically coupled (J = −218 cm^{-1}). Oxidation of the μ-oxo species in aqueous solution with $Na_2S_2O_8$ affords the orange-brown mixed-valence species $[L_2Ru^{III}Ru^{IV}(\mu\text{-}O)(\mu\text{-}CH_3CO_2)_2](PF_6)_3$; the crystal structure of the diperchlorate hexafluorophosphate salt has been determined by X-ray crystallography. Crystal data: monoclinic; $C2/c$ (C^6_{2h}, No. 15); a = 35.270 (6), b = 10.661 (2), c = 21.650 (4) Å; β = 114.43 (1)°; V = 7411 Å^3; ρ_{calcd} = 1.83 g/cm^3; Z = 8. The overall structure is as in the (μ-oxo)bis(μ-acetato)diruthenium(III) species; the corresponding Ru–N and Ru–O distances are shorter, but the Ru···Ru distance *increases* by 0.084 Å. This is in contrast to the prediction based on a simple metal–metal-bonding model, where the Ru^{III}_2 dimer has a Ru–Ru bond of order 1.0 ($\sigma^2\pi^4\pi^{*4}$) that increases upon oxidation to 1.5 ($\sigma^2\pi^4\pi^{*3}$). From a comparison with analogous complexes of V(III) and Fe(III), it is concluded that no metal–metal bonds exist. Electronic and ^{1}H and ^{13}C NMR spectra, magnetic properties, and the electrochemistry in protic and aprotic solvents of these new compounds are reported.

Introduction

In recent years, the structural, electronic, and magnetic properties of (μ-hydroxo)bis(μ-carboxylato)dimetal[2-6] complexes and their (μ-oxo)bis(μ-carboxylato)dimetal[7-14] analogues have been intensively studied. This interest has been stimulated by the discovery that these cores occur in the active sites of a number of non-heme iron metalloproteins[15] and probably in—at least two—manganese-containing enzymes.[16,17]

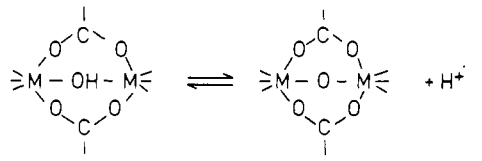

Subsequently, and as consequence of this, a fast growing series of low molecular weight first-row transition-metal complexes of this type have been synthesized and structurally characterized.[2-14] These include homo- and heterobimetallic[4] complexes and a number of mixed-valence species of the types $M^{III}M^{II}$ and $M^{III}M^{IV}$.[5,10,11,13] The metal–metal distances in these complexes are usually in the range 3.1–3.6 Å, and in no instance has evidence for direct metal–metal bonding been found.

We have now initiated a program systematically investigating complexes of this type that contain second-row transition metals. Second-row transition metals are known to readily form metal–metal bonds if two such metal ions can be brought into close enough proximity. Recently, we have shown[18] that $[L_2Mo^{III}_2(\mu\text{-}OH)(\mu\text{-}CH_3CO_2)_2]^{3+}$ is a classical Werner-type complex with strong antiferromagnetic coupling of the Mo^{III} centers (d^3–d^3). It has a Mo···Mo distance of 3.555 (1) Å, which excludes direct metal–metal bonding. Upon deprotonation of this species at the hydroxo bridge the diamagnetic μ-oxo-bridged complex $[L_2Mo^{III}_2(\mu\text{-}O)(\mu\text{-}CH_3CO_2)_2]^{2+}$ forms, which contains a short Mo–Mo distance of 2.885 (1) Å that has been assigned to a bond order 3 ($\sigma^2\pi^4$). Oxidation of this species yields the mixed-valence complex $[L_2Mo^{III}Mo^{IV}(\mu\text{-}O)(\mu\text{-}CH_3CO_2)_2]^{3+}$ with a slightly longer Mo–Mo bond of 2.969 (1) Å of the order 2.5 ($\sigma^2\pi^3$).[18b]

Following this simple concept of metal–metal bonding for a core with C_{2v} symmetry,[39-42] it appeared to be interesting to develop the analogous chemistry of ruthenium. At the outset it was expected that in (μ-oxo)bis(μ-carboxylato)diruthenium(III) complexes the Ru–Ru bond would be of the order 1 ($\sigma^2\pi^4\pi^{*4}$) and that oxidation to the $Ru^{III}Ru^{IV}$ species should increase the bond order to 1.5 ($\sigma^2\pi^4\pi^{*3}$) and, therefore, the Ru–Ru distance should decrease. We will show here that although the chemistry of (μ-oxo)bis(μ-carboxylato)diruthenium complexes is readily developed and closely follows the observations described for the molybdenum analogues, the understanding of the observed metal–metal distances in the Ru^{III}_2 dimer (3.258 (1) Å) and the $Ru^{III}Ru^{IV}$ mixed-valence species (3.342 (1) Å) is not straightforward and poses interesting questions. A preliminary communication describing some aspects of this work has been published.[19]

(1) (a) Ruhr-Universität. (b) Universität Heidelberg.
(2) Chaudhuri, P.; Wieghardt, K.; Nuber, B.; Weiss, J. *Angew. Chem., Int. Ed. Engl.* **1985**, *24*, 778.
(3) Armstrong, W. H.; Lippard, S. J. *J. Am. Chem. Soc.* **1984**, *106*, 4632.
(4) Chaudhuri, P.; Winter, M.; Küppers, H.-J.; Wieghardt, K.; Nuber, B.; Weiss, J. *Inorg. Chem.* **1987**, *26*, 3302.
(5) Wieghardt, K.; Bossek, U.; Bonvoisin, J.; Beauvillain, P.; Girerd, J. J.; Nuber, B.; Weiss, J.; Heinze, J. *Angew. Chem., Int. Ed. Engl.* **1986**, *25*, 1030.
(6) Siebert, H.; Tremmel, G. *Z. Anorg. Allg. Chem.* **1972**, *390*, 292.
(7) Armstrong, W. H.; Lippard, S. J. *J. Am. Chem. Soc.* **1983**, *105*, 4837.
(8) Wieghardt, K.; Pohl, K.; Gebert, W. *Angew. Chem., Int. Ed. Engl.* **1983**, *22*, 727.
(9) Wieghardt, K.; Bossek, U.; Ventur, D.; Weiss, J. *J. Chem. Soc., Chem. Commun.* **1985**, 347.
(10) Sheats, J. E.; Czernuszewicz, R. S.; Dismukes, G. C.; Rheingold, A. L.; Petrouleas, V.; Stubbe, J.; Armstrong, W. H.; Beer, R. H.; Lippard, S. J. *J. Am. Chem. Soc.* **1987**, *109*, 1435.
(11) (a) Wieghardt, K.; Köppen, M.; Nuber, B.; Weiss, J. *J. Chem. Soc., Chem. Commun.* **1986**, 1530. (b) Köppen, M.; Fresen, G.; Wieghardt, K.; Llusar, R.; Nuber, B.; Weiss, J. *Inorg. Chem.* **1988**, *27*, 721.
(12) Armstrong, J. E.; Robinson, E. R.; Walton, R. A. *Inorg. Chem.* **1983**, *22*, 1301.
(13) Hartman, J.; Rardin, R. L; Chaudhuri, P.; Pohl, K.; Wieghardt, K.; Nuber, B.; Weiss, J.; Papaefthymiou, G. C.; Frankel, R. B.; Lippard, S. J. *J. Am. Chem. Soc.* **1987**, *109*, 7387.
(14) Alcock, N. W.; Bartlett, P. N.; Gordon, D.; Illson, T. F.; Wallbridge, M. G. H. *J. Chem. Soc., Chem. Commun.* **1986**, 614.
(15) Lippard, S. J. *Angew. Chem., Int. Ed. Engl.* **1988**, *27*, 353.
(16) (a) Kono, Y.; Fridovich, I. *J. Biol. Chem.* **1983**, *258*, 6015, 13646. (b) Beyer, W. F.; Fridovich, I. *Biochemistry* **1985**, *24*, 6460.
(17) Willing, A.; Follmann, H.; Auling, G. *Eur. J. Biochem.* **1988**, *170*, 603.
(18) (a) Neves, A.; Bossek, U.; Wieghardt, K.; Nuber, B.; Weiss, J. *Angew. Chem., Int. Ed. Engl.* **1988**, *27*, 685. (b) Neves, A.; Bossek, U.; Wieghardt, K., Nuber, B.; Weiss, J. *Inorg. Chem.*, in press.
(19) Neubold, P.; Wieghardt, K.; Nuber, B.; Weiss, J. *Angew. Chem., Int. Ed. Engl.* **1988**, *27*, 933.

0020-1669/89/1328-0459$01.50/0

Interestingly, Walton et al.[20] have recently described an Os(IV) dimer containing the $[Os_2(\mu\text{-}O)(\mu\text{-}CH_3CO_2)_2]^{4+}$ core with an Os···Os distance of 3.440 (2) Å. These authors have left open the question as to whether a direct metal–metal bond exists or not.

Experimental Section

The ligand 1,4,7-trimethyl-1,4,7-triazacyclononane (L)[21] and the starting complex $Ru(dmso)_4Cl_2$[22] (dmso = dimethyl sulfoxide) have been prepared according to procedures described in the literature.

$[LRuCl_3]\cdot H_2O$. To a suspension of $RuCl_2(dmso)_4$ (1.0 g; 2.1 mmol) in absolute ethanol (25 mL) was added 1,4,7-trimethyl-1,4,7-triazacyclononane (0.8 g; 8 mmol). After 30 min of stirring at 60 °C, the solution was refluxed for 2 h. The solvent was then removed under reduced pressure, and the resulting red-orange residue was refluxed with concentrated HCl (20 mL) for 30 min. Orange microcrystals precipitated. The yield improved upon reduction of the reaction volume to half (yield 0.49 g, 60%).

Anal. Calcd for $(C_9H_{21}N_3)RuCl_3\cdot H_2O$: C, 27.3; H, 5.8; N, 10.6. Found: C, 27.5; H, 5.8; N, 10.5.

$[L_2Ru_2(\mu\text{-}O)(\mu\text{-}R\text{-}CO_2)_2](PF_6)_2$. The preparation of the (μ-oxo)bis(μ-carboxylato)diruthenium(III) complexes was accomplished by following a general procedure. A suspension of $[LRuCl_3]\cdot H_2O$ (0.25 g; 0.6 mmol) in an aqueous solution (15 mL) containing the sodium salt of the respective carboxylic acid (1.0 g in all cases; the pH of the solution was adjusted to 7) was refluxed for 30 min until a clear purple solution was obtained. To this hot solution was added $NaPF_6$ (0.75 g) dissolved in water (10 mL). Upon cooling of the solution to 0 °C for 12 h, purple crystals of the desired product formed. The yields varied between 30 and 90%, depending on the carboxylic acid used.

Anal. Calcd for $[(C_9H_{21}N_3)_2Ru_2O(CH_3CO_2)_2](PF_6)_2$: C, 27.3; H, 5.1; N, 8.7. Found: C, 27.1; H, 5.0; N, 8.6. Calcd for $[(C_6H_{21}N_3)_2Ru_2O(HCOO)_2](PF_6)_2$: C, 25.6; H, 4.7; N, 8.9. Found: C, 25.8; H, 4.8; N, 8.7. Calcd for $[(C_9H_{21}N_3)_2Ru_2O(CF_3CO_2)_2](PF_6)_2$: C, 24.5; H, 4.0; N, 7.8. Found: C, 24.2; H, 3.8; N, 7.7. Calcd for $[(C_9H_{21}N_3)_2Ru_2O(C_6H_5CO_2)_2](PF_6)_2$: C, 35.2; H, 4.8; N, 7.7. Found: C, 35.4; H, 4.8; N, 7.4. Calcd for $[(C_9H_{21}N_3)_2Ru_2O(CCl_3CO_2)_2](PF_6)_2$: C, 22.5; H, 3.6; N, 7.1. Found: C, 22.3; H, 3.6; N, 6.8. Calcd for $[(C_9H_{21}N_3)_2Ru_2O(CH_2ClCO_2)_2](PF_6)_2$: C, 25.5; H, 4.5; N, 8.1. Found: C, 25.3; H, 4.4; N, 8.2.

$[L_2Ru_2(\mu\text{-}OH)(\mu\text{-}CH_3CO_2)_2](PF_6)_3$. Purple $[L_2Ru_2(\mu\text{-}O)(\mu\text{-}CH_3CO_2)_2](PF_6)_2$ (0.10 g; 0.1 mmol) was dissolved in 2 M HCl (5 mL) at 20 °C. A color change from purple to green was observed. Addition of $NaPF_6$ (0.15 g) dissolved in 2 M HCl (5 mL) initiated the precipitation of green microcrystals at 0 °C (yield 95%).

Anal. Calcd for $[(C_9H_{21}N_3)_2Ru_2(OH)(CH_3CO_2)_2](PF_6)_3$: C, 23.7; H, 4.4; N, 7.5. Found: C, 24.0; H, 4.5; N, 7.6.

$[L_2Ru_2(\mu\text{-}O)(\mu\text{-}CH_3CO_2)_2](PF_6)_3$. To a solution of $[L_2Ru_2(\mu\text{-}O)(\mu\text{-}CH_3CO_2)_2](PF_6)_2$ (0.15 g; 0.15 mmol) in water (10 mL) was added $Na_2S_2O_8$ (0.10 g) dissolved in water (2 mL), whereupon the color of the solution changed to brown. Addition of $NaPF_6$ (0.20 g) dissolved in water (3 mL) initiated the precipitation of brown microcrystals (yield 94%).

Single crystals suitable for X-ray crystallography of $[L_2Ru_2(\mu\text{-}O)(\mu\text{-}CH_3CO_2)_2](ClO_4)_2(PF_6)$ were grown from an aqueous solution of the PF_6 salt to which $NaClO_4\cdot H_2O$ was added. *Caution!* Perchlorate salts of Ru^{III} complexes are potentially very hazardous especially when heated; they are explosive.

This salt was only prepared in very small quantities (≈20 mg) in order to obtain a few single crystals for X-ray analysis.

Electrochemistry. Electrochemical experiments were performed with a Princeton Applied Research (PAR) Model 173 potentiostat, a PAR Model 175 universal programmer, a Model 179 digital coulometer, and a Kipp & Zonen X-Y recorder. Cyclic voltammograms (CV's) were made on acetonitrile and/or aqueous solutions containing 0.1 M tetra-*n*-butylammonium hexafluorophosphate ((TBA)PF_6) in the former case or a series of buffers in the latter as supporting electrolyte, and experiments were conducted at 22 °C under an argon atmosphere. A standard three-electrode system was used, comprising a glassy-carbon (aqueous solution) or a platinum-button (CH_3CN) working electrode, a platinum-wire electrode, and an Ag/AgCl (saturated LiCl in ethanol) reference electrode. The performance of the reference electrode was monitored by measuring the Fe(+1/0) couple of ferrocene (+0.537 V vs Ag/AgCl).[26] Formal redox potentials in acetonitrile ($E_{1/2}$ values taken as $(E_{p,a} + E_{p,c})/2$) are given versus the normal hydrogen electrode (NHE); they were calculated by subtracting 0.14 V from the values measured versus the Ag/AgCl reference electrode.[26] The pH dependence of redox potentials in aqueous solutions was measured by using a HCl/KCl or a citric acid/NaOH buffer. The concentration of complexes was $\approx 10^{-3}$ M. Diagnostic criteria for the reversibility of the electron-transfer processes were employed in the usual manner.[27] Scan rates of CV's were between 20 and 200 mV s^{-1}.

Table I. Crystallographic Data for $[L_2Ru_2(\mu\text{-}O)(\mu\text{-}CH_3CO_2)_2](PF_6)_2\cdot 0.5H_2O$ and $[L_2Ru_2(\mu\text{-}O)(\mu\text{-}CH_3CO_2)_2](ClO_4)_2(PF_6)$

chem formula	$[C_{22}H_{48}N_6O_5Ru_2]$-$(PF_6)_2\cdot 0.5H_2O$	$[C_{22}H_{48}N_6O_5Ru_2]$-$(ClO_4)_2(PF_6)$
fw	977.7	1022.6
space group	*Ibca* (No. 73)	*C*2/*c* (No. 15)
a, Å	13.631 (4)	35.270 (6)
b, Å	14.992 (8)	10.661 (2)
c, Å	35.465 (14)	21.650 (4)
β, deg		114.43 (1)
ρ_{calcd}, g cm^{-3}	1.79	1.83
T, °C	22	22
λ, Å	0.7107	0.7107
V, Å^3	7247.5	7411
Z	8	8
μ, cm^{-1}	10.1	10.8
transmission coeff	0.8–1.0	0.82–1.0
R^a	0.041	0.047
$R_w{}^b$	0.038	0.052

$^a R = \sum||F_o| - |F_c||/\sum|F_o|$. $^b R_w = [\sum w(|F_o| - |F_c|)^2/\sum w|F_o|^2]^{1/2}$, $w = 1/\sigma^2(I)$.

Physical Measurements. Electronic absorption spectra in the 200–1400-nm range were recorded with a Perkin-Elmer Lambda 9 spectrophotometer, while the infrared spectra (KBr disks) were recorded with a Perkin-Elmer Model 283B spectrophotometer. Magnetic susceptibilities of powdered samples were recorded on a Faraday-type magnetic balance (Bruker research magnet, Sartorius microbalance, and Bruker B-VT 1000 automatic temperature control in the temperature range 98–293 K). Diamagnetic corrections were applied in the usual manner with use of tabulated Pascal's constants. The ^1H NMR spectra were recorded in the FT mode with a Bruker AM-400 spectrometer at a magnetic field of 400.1 MHz, and the ^{13}C NMR spectra, at a field of 100.6 MHz. Samples were dissolved in acetone-d_6, and resonances were usually referenced internally to that of tetramethylsilane.

X-ray Crystallography. A purple, prismatic crystal of $[L_2Ru_2(\mu\text{-}O)(\mu\text{-}CH_3CO_2)_2](PF_6)_2\cdot 0.5H_2O$ and a brown prismatic crystal of $[L_2Ru_2(\mu\text{-}O)(\mu\text{-}CH_3CO_2)_2](ClO_4)_2(PF_6)$ were attached to glass fibers and mounted on a four-circle diffractometer. The unit cell dimensions were obtained by a least-squares fit of 25 reflections ($3.8 < 2\theta < 30°$). The data are summarized in Table I. Intensity data were corrected for Lorentz and polarization effects in the usual manner; empirical absorption corrections (ψ scans of seven reflections, $5.2 < 2\theta < 40.8°$, for each crystal) were also carried out.[23] The function minimized during least-squares refinement was $\sum w(|F_o| - |F_c|)^2$. The structures were solved via conventional Patterson and Fourier syntheses. Neutral-atom scattering factors and anomalous dispersion corrections for non-hydrogen atoms were taken from ref 24, and hydrogen atom scattering factors, from ref 25. The positions of methyl (rigid-body refinement) and methylene protons were calculated (d(C–H) = 0.96 Å, sp^3-hybridized carbon) and were included in the final refinement cycle with isotropic thermal parameters. All non-hydrogen atoms were defined with use of anisotropic displacement parameters with the exception of the oxygen atoms of one disordered ClO_4^- anion in $[L_2Ru_2(\mu\text{-}O)(\mu\text{-}CH_3CO_2)_2](ClO_4)_2(PF_6)$, for which isotropic thermal parameters were used.

Results

Syntheses. A quite general synthetic route to complexes containing the (μ-oxo)bis(μ-carboxylato)dimetal core is the hydrolysis

(20) Armstrong, J. W.; Robinson, W. R.; Walton, R. A. *Inorg. Chem.* **1983**, *22*, 1301.
(21) Wieghardt, K.; Chaudhuri, P.; Nuber, B.; Weiss, J. *Inorg. Chem.* **1982**, *21*, 3086.
(22) Evans, I. P.; Spencer, A.; Wilkinson, G. *J. Chem. Soc., Dalton Trans.* **1973**, 204.
(23) All computations were carried out on an ECLIPSE computer using the SHELXTL program package.
(24) *International Tables for X-ray Crystallography*; Kynoch: Birmingham, England, 1974; Vol. IV, pp 99, 149.
(25) Stewart, R. F.; Davidson, E. R.; Simpson, W. T. *J. Chem. Phys.* **1965**, *42*, 3175.
(26) (a) Gagné, R. R.; Koval, C. A.; Lisensky, G. C. *Inorg. Chem.* **1980**, *19*, 2854. (b) Gritzner, G.; Kuta, J. *Pure Appl. Chem.* **1982**, *54*, 1527.
(27) Nicholson, R. S.; Shain, I. *Anal. Chem.* **1964**, *36*, 706.

Table II. Electronic[a] and IR[b] Spectral Data

complex	λ_{max}, nm (ϵ, L mol^{-1} cm^{-1})	ν_{as}(CO), cm^{-1}	ν_s(CO), cm^{-1}
$[L_2Ru_2(\mu\text{-}O)(\mu\text{-}CH_3CO_2)_2](PF_6)_2$	542 (6.1 × 10^3), 340 sh, 288 (8.7 × 10^3), 232 (8.0 × 10^3)	1548	1425
$[L_2Ru_2(\mu\text{-}O)(\mu\text{-}CF_3CO_2)_2](PF_6)_2$	546 (6.1 × 10^3), 340 sh, 261 (10.2 × 10^3)	1645	1468
$[L_2Ru_2(\mu\text{-}O)(\mu\text{-}HCO_2)_2](PF_6)_2$	544 (5.9 × 10^3), 340 sh, 289 (7.8 × 10^3), 239 (7.0 × 10^3)	1566	1345
$[L_2Ru_2(\mu\text{-}O)(\mu\text{-}PhCO_2)_2](PF_6)_2$	549 (5.1 × 10^3), 279 (16.3 × 10^3)	1535	1397
$[L_2Ru_2(\mu\text{-}O)(\mu\text{-}Cl_3CCO_2)_2](PF_6)_2$	551 (5.5 × 10^3), 340 sh, 276 (12.1 × 10^3)	1631	1361
$[L_2Ru_2(\mu\text{-}O)(\mu\text{-}H_2ClCCO_2)_2](PF_6)_2$	545 (6.0 × 10^3), 340 sh, 287 (8.3 × 10^3), 250 (7.9 × 10^3)	1584	1411
$[L_2Ru_2(\mu\text{-}OH)(\mu\text{-}CH_3CO_2)_2](PF_6)_3$	585 (730), 470 (2.5 × 10^3), 277 (3.8 × 10^3)	1550	1433
$[L_2Ru_2(\mu\text{-}O)(\mu\text{-}CH_3CO_2)_2](PF_6)_3$	478 (5.7 × 10^3), 334 (10.0 × 10^3), 1591 (276)	1530/1500	1426

[a] Measured in CH_3CN at 22 °C (ϵ are given per dimer). [b] KBr disks.

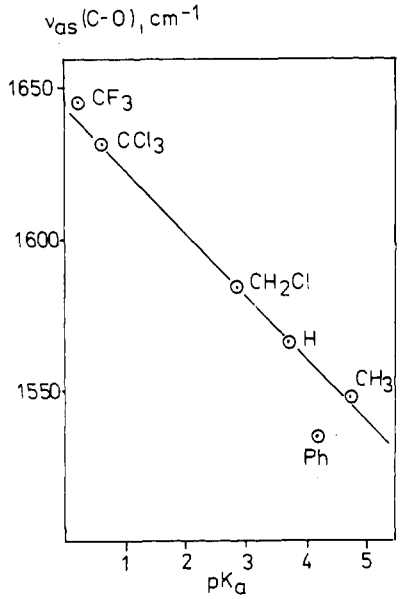

Figure 1. Correlation between the ν_{as}(CO) stretching frequency of $[L_2Ru_2(\mu\text{-}O)(\mu\text{-}R\text{-}CO_2)_2](PF_6)_2$ complexes and the pK_a values of the uncoordinated carboxylic acid.

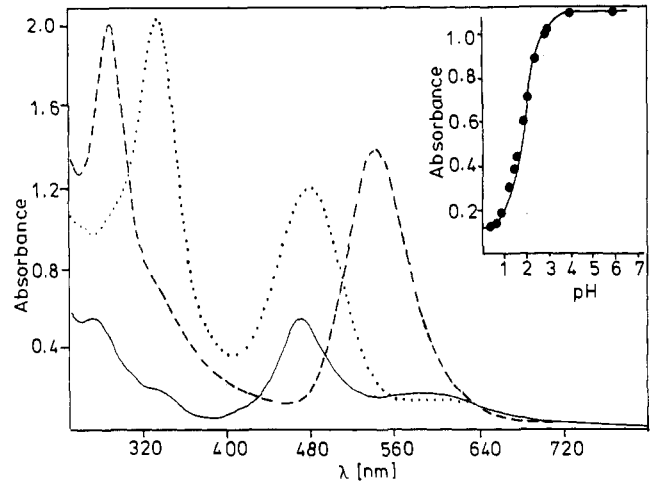

Figure 2. Electronic spectra of $[L_2Ru_2(\mu\text{-}O)(\mu\text{-}CH_3CO_2)_2](PF_6)_2$ (---; 2.15 × 10^{-4} M in H_2O), $[L_2Ru_2(\mu\text{-}OH)(\mu\text{-}CH_3CO_2)_2](PF_6)_3$ (—; 2.15 × 10^{-4} M in 5 M HCl), and $[L_2Ru_2(\mu\text{-}O)(\mu\text{-}CH_3CO_2)_2](PF_6)_3$ (···; 2.15 × 10^{-4} M in H_2O) (1-cm cell). The inset shows the absorption of $[L_2Ru_2(\mu\text{-}O)(\mu\text{-}CH_3CO_2)_2]^{2+}$ at 540 nm as a function of pH.

of monomeric LMX_3 species (X = Cl, Br; M = Fe^{III},[8,13] Mn^{III},[9] V^{III},[11] Mo^{III},[18] L = a tridentate macrocyclic N donor) in aqueous solution containing sodium acetate (or other carboxylates). The starting complex $LRu^{III}Cl_3\cdot H_2O$ (L = 1,4,7-trimethyl-1,4,7-triazacyclononane) is readily available from the reaction of Ru(dmso)$_4Cl_2$ (dmso = dimethyl sulfoxide)[22] and L in absolute ethanol. After refluxing of this suspension and removal of the solvent, the residue was heated with concentrated HCl in the presence of air. Orange $LRuCl_3\cdot H_2O$ was obtained in 60% yield. The effective magnetic moments of 2.35 μ_B at 293 K and 1.94 μ_B at 100 K are in agreement with an octahedral d^5 low-spin complex of Ru^{III}. The CV (0.1 M (TBA)PF_6; CH_3CN; 22 °C; Pt working electrode) exhibits a reversible one-electron wave at +1.18 V vs NHE and an irreversible reduction at −0.59 V in the potential range +1.9 to −1.6 V vs Ag/AgCl. This indicates an oxidation to $[LRuCl_3]^+$ and an irreversible reduction (eq 1).

$$[LRuCl_3]^+ + e^- \rightleftharpoons LRu^{III}Cl_3 \xrightarrow{+e^-} \text{reduced product} \quad (1)$$

Hydrolysis of $LRuCl_3\cdot H_2O$ in aqueous solutions containing the sodium salts of a variety of carboxylic acids at elevated temperatures yielded deep purple solutions from which upon addition of solid $NaPF_6$ the purple, microcrystalline complexes $[L_2Ru^{III}_2(\mu\text{-}O)(\mu\text{-}RCO_2)_2](PF_6)_2$ precipitated (R = H, CH_3, CF_3, CCl_3, CH_2Cl, C_6H_5). It is noted that Sasaki et al.[28] have prepared the complex $[(py)_6Ru_2(\mu\text{-}O)(\mu\text{-}CH_3CO_2)_2](PF_6)_2$ (py = pyridine) and Meyer et al.[29] have obtained $[(tpm)_2Ru_2(\mu\text{-}O)(\mu\text{-}CH_3CO_2)_2]^{2+}$ (tpm = tripyrazolylmethane); both compounds contain the (μ-oxo)bis(μ-acetato)diruthenium(III) core. Interestingly, the ν_{as}(C–O) stretching frequency of these (μ-oxo)bis(μ-carboxylato)diruthenium(III) complexes (Table II) decreases with increasing pK_a value of the uncoordinated free carboxylic acid (Figure 1). Similar linear relationships have previously been observed for bis(μ-hydroxo)bis(μ-carboxylato)dicobalt(III) complexes[30] and their chromium(III) analogues;[31] they are an indication of the electron-withdrawing capacity of the R group of the respective carboxylic acid. The same correlation may be constructed by using Taft's inductive parameter σ_I.[33]

When the purple (μ-oxo)bis(μ-carboxylato)diruthenium(III) species are dissolved in 2 M HCl, a color change to green occurs. Addition of $NaPF_6$ to such a solution of the bis(μ-acetato) complex afforded green crystals of $[L_2Ru^{III}_2(\mu\text{-}OH)(\mu\text{-}CH_3CO_2)_2](PF_6)_3$, a protonated complex containing the (μ-hydroxo)bis(μ-acetato)diruthenium(III) core (eq 2). Spectrophotometric de-

$$[L_2Ru_2(\mu\text{-}O)(\mu\text{-}CH_3CO_2)_2]^{2+} + H^+ \overset{K_a^{-1}}{\rightleftharpoons} [L_2Ru_2(\mu\text{-}OH)(\mu\text{-}CH_3CO_2)_2]^{3+} \quad (2)$$

termination of the dissociation constant, K_a, yielded a pK_a value of 1.9 ± 0.1 at 25 °C (I = 1.0 M), as is shown in the inset of Figure 2. pH-dependent CV's measured in aqueous solution yielded the same value within experimental error (see below).

In the infrared spectrum of $[L_2Ru_2(\mu\text{-}OH)(\mu\text{-}CH_3CO_2)_2](PF_6)_3$ the presence of the μ-OH bridge is clearly established by a sharp O–H stretching frequency at 3544 cm^{-1}.

(28) Sasaki, Y.; Suzuki, M.; Tokiwa, A.; Ebihara, M.; Yamaguchi, T.; Kabuto, C.; Ito, T. *J. Am. Chem. Soc.* **1988**, *110*, 6251.
(29) Llobet, A.; Curry, M. E.; Evans, H. T.; Meyer, T. J. Submitted for publication.
(30) Wieghardt, K. *J. Chem. Soc., Dalton Trans.* **1973**, 2548.
(31) Springborg, J.; Toftlund, H. *Acta Chem. Scand.* **1979**, *A33*, 31.
(32) Baumann, J. A.; Salmon, D. J.; Wilson, S. T.; Meyer, T. J.; Hatfield, W. E. *Inorg. Chem.* **1978**, *17*, 3342.
(33) Values for Taft's inductive parameters, σ_I, were taken from: *Correlation Analysis in Chemistry*; Plenum Press: New York and London, 1978; Chapter 10. Values for acid dissociation constants, pK_a, were taken from: Kortüm, G.; Vogel, W.; Andrussow, K. *Dissociation Constants of Organic Acids in Aqueous Solutions*; Butterworths: London, 1961.

Scheme I

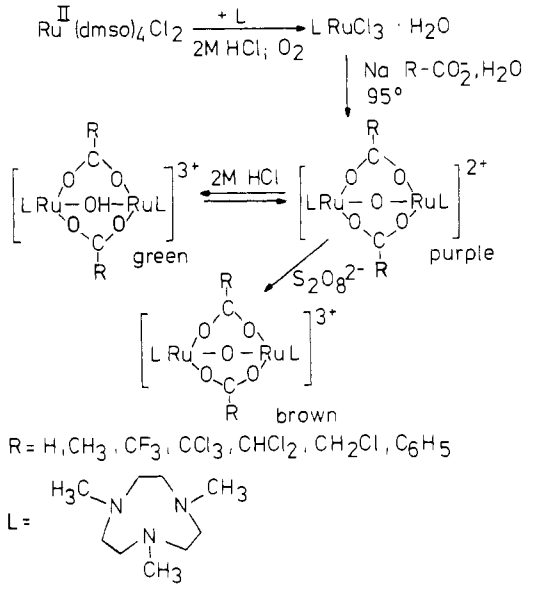

The oxidation of the (μ-oxo)bis(μ-carboxylato)diruthenium(III) complexes with $Na_2S_2O_8$ in aqueous solution yields the brown mixed-valence $Ru^{III}Ru^{IV}$ complexes $[L_2Ru_2(\mu\text{-}O)(\mu\text{-}RCO_2)_2]^{3+}$. The tris(hexafluorophosphate) salt of the bis(μ-acetato) complex was isolated, and the crystal structure of $[L_2Ru_2(\mu\text{-}O)(\mu\text{-}CH_3CO_2)_2](ClO_4)_2(PF_6)$ has been determined by X-ray crystallography (see below). Scheme I summarizes the preparations described in this work.

Electronic Spectra and Magnetic Properties. Figure 2 shows the electronic spectra of the (μ-oxo)bis(μ-acetato)diruthenium(III) complex, its protonated μ-hydroxo analogue, and the mixed-valence μ-oxo complex in the 300–800-nm range. Data for the other complexes are given in Table II. The electronic spectra of all (μ-oxo)bis(μ-carboxylato)diruthenium(III) complexes known to date are very similar regardless of the nature of the capping ligands; they exhibit three very intense absorption maxima at 540–580, ≈290, and 232 nm with molar extinction coefficients $>10^3$ L mol^{-1} cm^{-1}. In addition, in some instances a shoulder at 340 nm has been detected.

The first of these low-energy absorptions is assigned to a transition between MO's of the Ru dπ and oxygen pπ orbitals of the Ru–O–Ru moiety.[32] This is nicely corroborated by the fact that the absorption spectrum of the protonated form is quite different (Figure 2). The intensity of the absorption in the visible region at 540 nm is markedly reduced (by a factor of 8). Removal of one electron from the (μ-oxo)bis(μ-acetato)diruthenium(III) core to generate the mixed-valence dimer leads to a small shift of the intense Ru–O–Ru charge-transfer (CT) band in the visible region to a smaller wavelength whereas the CT band at 288 nm is shifted to a higher wavelength of 334 nm (Figure 2). A broad absorption at 1591 nm (ϵ = 276) is observed, which is assigned to an intervalence charge-transfer transition. A similar band has been reported for Walton's $Os^{III}Os^{IV}$ mixed-valence complex at 1060 nm ($\epsilon \approx 500$).[20]

Measurements of the molar susceptibility of (μ-oxo)bis(μ-carboxylato)diruthenium(III) complexes show these materials to be diamagnetic, as do the ^{1}H NMR measurements (see below). This is an important feature of these complexes, since the majority of known Ru^{III}–O–Ru^{III} species are paramagnetic at room temperature with magnetic moments of approximately 1.8 μ_B/Ru^{III} and intramolecular antiferromagnetic spin-exchange coupling (singlet ground state).[34]

In contrast, the μ-OH-bridged complex $[L_2Ru_2(\mu\text{-}OH)(\mu\text{-}CH_3CO_2)_2](PF_6)_3$ is paramagnetic at 293 K with a magnetic moment of 1.3 μ_B/Ru^{III} ion that decreases to 0.5 μ_B/Ru at 98 K. Thus, an antiferromagnetic intramolecular spin coupling is observed. The temperature-dependent susceptibility in the temperature range 100–293 K was calculated by using the general isotropic exchange Hamiltonian, $H = -2JS_1 \cdot S_2$, for $S_1 = S_2 = {}^1/_2$. A least-squares fit yielded $J = -218 \pm 5$ cm^{-1} and $g = 2.4$ (TIP = 0). Typically, g values for Ru(III) are highly anisotropic, with average values varying from about 2.3 to 2.0.[34] For $[(bpy)_2(NO_2)RuORu(NO_2)(bpy)_2](PF_6)_2$ a g value of 2.48 has been reported.[33] Thus, the calculated g of 2.4 for the present case is not unreasonable.

The magnetic moment of $[L_2(Ru_2(\mu\text{-}O)(\mu\text{-}CH_3CO_2)_2](PF_6)_3$ is slightly temperature dependent; it varies from 1.31 μ_B/Ru at 98 K to 1.43 μ_B/Ru at 298 K. The magnetic moment of 2.02 μ_B/Ru dimer at room temperature agrees well with values reported for binuclear Ru(II)/Ru(III) mixed-valence species, indicating the presence of one unpaired electron per dimer.

^{1}H and ^{13}C NMR Spectra. The 400-MHz ^{1}H NMR spectrum of $[L_2Ru_2(\mu\text{-}O)(\mu\text{-}CH_3CO_2)_2](PF_6)_2$ in acetone-d_6 at ambient temperature shows signals for each methylene proton of the cyclic amine, two signals (ratio 2:1) for the methyl protons of N-methyl groups, and one signal for the protons of the acetato bridges (Table III).

In crystals of $[L_2Ru_2(\mu\text{-}O)(\mu\text{-}CH_3CO_2)_2](PF_6)_2 \cdot 0.5H_2O$ the ring conformations of both coordinated triamines of a given cation are identical; they are either both ($\lambda\lambda\lambda$)($\lambda\lambda\lambda$) or both ($\delta\delta\delta$)($\delta\delta\delta$), and since the space group is D_{2h}^{27} (*Ibca*), both enantiomers are present in equal amounts—the racemate crystallizes out and, consequently, the racemate is present in solution upon dissolving the crystals of $[L_2Ru_2(\mu\text{-}O)(\mu\text{-}CH_3CO_2)_2](PF_6)_2 \cdot 0.5H_2O$. In order to assign the ^{1}H signals, it suffices to consider the cation in an idealized C_{2v} symmetry (structure I) where both Ru atoms, the oxo bridge, and one N–CH_3 group of each coordinate triamine lie on the additional mirror plane.

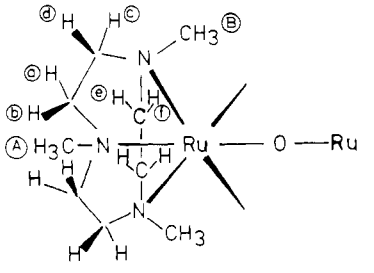

I

The methylene protons a, b, c, and d give rise to multiplets (Table III) that are composed of a doublet of a doublet of doublets with a vicinal coupling constant of 10–11 Hz and a geminal coupling constant of ~7 Hz. For protons e and f no geminal coupling has been observed, because two vicinal protons are identical due to the mirror plane perpendicular to the C_c–$C_{c'}$ bond (structure I, Table IV). The methyl protons B and A of the cyclic triamine exhibit two signals at δ = 1.35 and 3.78, which correspond to 12 H and 6 H, respectively; the signal of the acetato methyl

Table III. 400-MHz ^{1}H NMR Data for $[L_2Ru_2(\mu\text{-}O)(\mu\text{-}RCO_2)_2](PF_6)_2$ Complexes[a]

δ			
CH_3	CF_3	H	assgnt[b]
1.35 (12 H, s)	1.47 (12 H, s)	1.42 (12 H, s)	B
1.76 (6 H, s)			CH_3 acetato
2.24 (4 H, m)	2.47 (4 H, m)	2.28 (4 H, m)	c
3.51 (4 H, m)	3.50 (4 H, m)	3.48 (4 H, m)	d
3.65 (4 H, m)	3.82 (4 H, m)	3.75 (4 H, m)	a
3.78 (6 H, s)	3.61 (6 H, s)	3.76 (6 H, s)	A
3.96 (4 H, m)	3.95 (4 H, m)	3.96 (4 H, m)	f
4.20 (4 H, m)	4.35 (4 H, m)	4.24 (4 H, m)	e
4.54 (4 H, m)	4.75 (4 H, m)	4.59 (4 H, m)	b
		6.37 (2 H, s)	H formato

[a] Measured in acetone-d_6 at ambient temperature; m = multiplet, s = singlet. [b] For the labeling see structure I.

(34) Weaver, T. T.; Meyer, T. J.; Adeyemi, S. A.; Brown, G. M.; Eckbert, R. P.; Hatfield, W. E.; Johnson, E. C.; Murray, R. W.; Untereker, D. *J. Am. Chem. Soc.* **1975**, *97*, 3039.

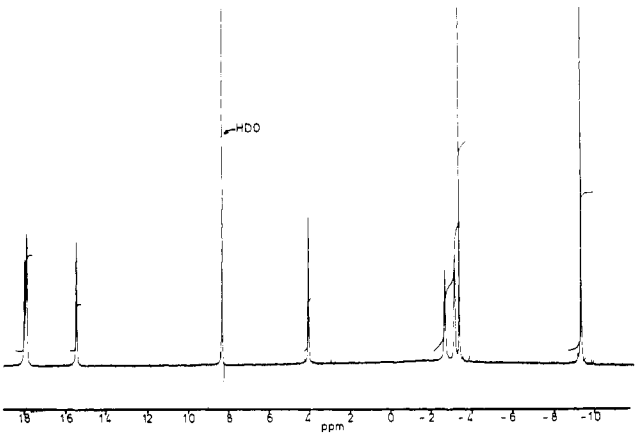

Figure 3. 400-MHz ^1H NMR spectrum of $[L_2Ru_2(\mu\text{-}OH)(\mu\text{-}CH_3CO_2)_2](PF_6)_3$ in DCl/D_2O (20%).

Table IV. 100-MHz ^{13}C NMR Data for $[L_2Ru_2(\mu\text{-}O)(\mu\text{-}RCO_2)_2](PF_6)_2$ Complexes[a]

δ			
CH_3	CF_3	H	assgnt[c]
23.9			$H_3C\text{-}CO_2^-$
54.9	55.2	55.0	B
54.6	56.7	55.3	A
59.9	61.8	60.3	a
63.8	67.7	64.6	b
63.8	64.0	63.8	c
193.1	*b*	*b*	$H_3C\text{-}CO_2^-$

[a] Measured in acetone-d_6. [b] Not observed. [c] Labeling:

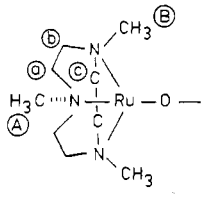

group is observed at $\delta = 1.76$ (6 H), which is absent in the ^1H NMR spectrum of the μ-formato and μ-trifluoroacetato complexes. The assignments given in Table III (structure I) were unambiguously established by the ^{13}C NMR spectrum (Table IV), a $^{13}C\text{-}^1H$ correlation, and a series of NOE difference spectra.

A comparison of the ^1H NMR spectra of the μ-acetato, μ-formato, and μ-trifluoroacetato complexes reveals that protons d and f resonate at the same frequencies whereas methylene protons a, b, d, and e and methyl protons A and B of the μ-formato complex resonate at frequencies intermediate between those of the μ-acetato and μ-trifluoroacetato complexes. "Axial" methylene protons b, d, and e are always more deshielded than "equatorial" methylene protons a, c, and f. This is probably due to an anisotropy effect of the bridging oxo and carboxylato groups.

Figure 3 shows the 400-MHz ^1H NMR spectrum of $[L_2Ru_2(\mu\text{-}OH)(\mu\text{-}CD_3CO_2)_2](PF_6)_3$ in 20% DCl/D_2O at ambient temperature. The spectrum consists of eight sharp resonances at −9.3, −3.4, −3.2, −2.6, +4.0, +15.4, +17.8 and +18.0 ppm. The same resonances have been observed for the undeuteriated complex $[L_2Ru_2(\mu\text{-}OH)(\mu\text{-}CH_3CO_2)_2](PF_6)_3$ in 20% DCl/D_2O, but an additional signal at +4.1 ppm has been detected that is assigned to the methyl protons of the μ-acetato bridges. This is reasonable since these methyl groups are furthest away from the paramagnetic Ru(III) centers and therefore least isotropically shifted, which is presumably a predominantly σ contact shift in nature. The μ-hydroxo complex may be considered as two separate $S = {}^1/_2$ Ru(III) systems, in which the dipolar contribution to the isotropic shifts (H/H_0) is negligible. If this assumption holds, the signals at −3.2, −2.6, and +4.0 ppm are assigned to equatorial methylene protons (pointing toward the bridging oxo and acetato groups; i.e., protons a, c, and f in structure I) whereas the more intense signals at −9.3 and −7.1 ppm are assigned to methyl protons B and A, respectively. Resonances at +15.4, +17.85, and +18.0 ppm should then belong to axial methylene protons b, d, and e. These assignments are of course tentative.

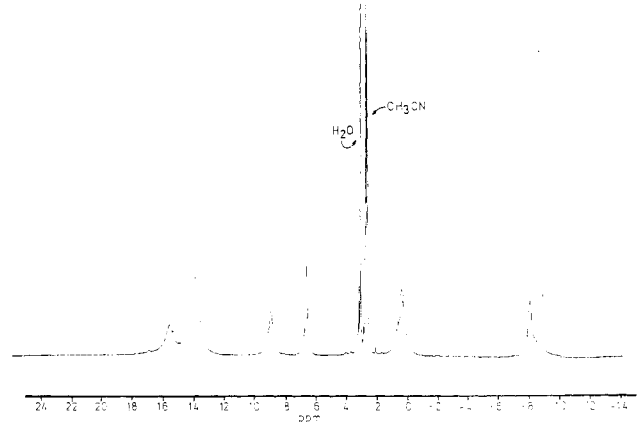

Figure 4. 400-MHz ^1H NMR spectrum of $[L_2Ru_3(\mu\text{-}O)(\mu\text{-}CH_3CO_2)_2](PF_6)_3$ in acetonitrile-d_3.

Table V. Atom Coordinates (×10⁴) and Temperature Factors (Å² × 10³) for $[L_2Ru_2(\mu\text{-}O)(\mu\text{-}CH_3CO_2)_2](PF_6)_2\cdot 0.5H_2O$

atom	x	y	z	U_{eq}[a]
Ru(1)	692 (1)	1614 (1)	1343 (1)	26 (1)
N(1)	2033 (3)	1818 (3)	1057 (1)	33 (1)
N(2)	489 (3)	610 (3)	934 (1)	35 (1)
N(3)	1533 (3)	583 (3)	1625 (1)	37 (1)
C(1)	1800 (4)	1564 (4)	658 (2)	44 (2)
C(2)	1299 (4)	670 (4)	648 (2)	47 (2)
C(3)	534 (4)	−234 (3)	1153 (2)	44 (2)
C(4)	1432 (4)	−263 (3)	1410 (2)	45 (2)
C(5)	2553 (4)	922 (4)	1610 (2)	43 (2)
C(6)	2816 (4)	1222 (4)	1219 (2)	42 (2)
C(7)	2370 (4)	2752 (3)	1068 (2)	43 (2)
C(8)	−473 (4)	648 (4)	743 (2)	47 (2)
C(9)	1233 (5)	437 (4)	2023 (2)	54 (2)
O(1)	0	2500	1076 (1)	27 (1)
O(2)	539 (2)	3778 (2)	1643 (1)	34 (1)
O(3)	1099 (2)	2422 (2)	1797 (1)	32 (1)
C(10)	1033 (4)	3251 (3)	1842 (1)	33 (2)
C(11)	1625 (4)	3647 (4)	2162 (2)	46 (2)
P(1)	0	7500	1936 (1)	39 (1)
F(11)	300 (3)	6486 (2)	1933 (1)	95 (2)
F(12)	0	7500	1505 (2)	178 (5)
F(13)	−1113 (3)	7272 (3)	1933 (2)	118 (2)
F(14)	0	7500	2367 (2)	131 (4)
P(2)	0	7500	295 (1)	55 (1)
F(21)	0	7500	−131 (2)	135 (4)
F(22)	763 (5)	6770 (5)	292 (2)	201 (4)
F(23)	0	7500	720 (2)	220 (6)
F(24)	810 (5)	8200 (5)	309 (2)	187 (4)
W(1)	2500	4089 (14)	0	167 (8)

[a] Equivalent isotropic U_{eq} defined as one-third of the trace of the orthogonalized U_{ij} tensor.

The 400-MHz ^1H NMR spectrum of the mixed-valence species $[L_2Ru_2(\mu\text{-}O)(\mu\text{-}CH_3CO_2)_2](PF_6)_3$ in CD_3CN at ambient temperature is remarkably different from the spectrum of the μ-hydroxo species (Figure 4). Seven broad resonances at −9.1, −8.1, +0.3, +6.5, +8.8, +13.7, and +15.4 ppm are observed with a line half-width of ≈0.3 ppm. In contrast, line half-widths for the antiferromagnetically coupled (μ-hydroxo)diruthenium(III) species are <0.05 ppm. In paramagnetic complexes the NMR line widths are governed by electron relaxation. In the antiferromagnetically coupled hydroxo-bridged Ru(III) dimer, the NMR lines are believed to be sharp because each low-spin d^5 center is relaxed by the presence of the other. In the Ru(III)–Ru(IV) dimer the Ru^{IV} center may be diamagnetic (on the NMR time scale) and, therefore, does not relax the unpaired electron on the other Ru(III) center; consequently, the NMR lines are broader.

Crystal Structures. The structure of the cation in $[L_2Ru_2(\mu\text{-}O)(\mu\text{-}CH_3CO_2)_2](PF_6)_2\cdot 0.5H_2O$, shown in Figure 5, consists of

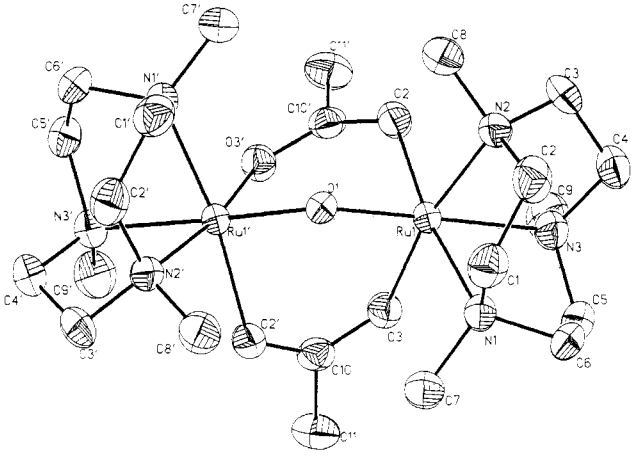

Figure 5. Structure of the cation of $[L_2Ru_2(\mu\text{-}O)(\mu\text{-}CH_3CO_2)_2](PF_6)_2\cdot 0.5H_2O$ and atom-labeling scheme.

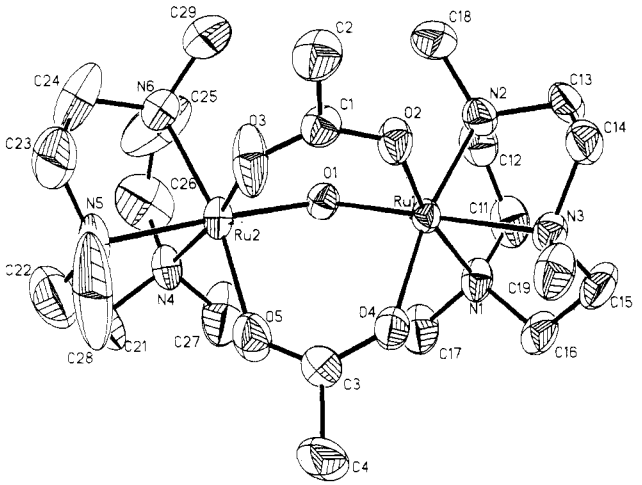

Figure 6. Structure of the cation of $[L_2Ru_2(\mu\text{-}O)(\mu\text{-}CH_3CO_2)_2](PF_6)_3$ and atom-labeling scheme.

Table VI. Bond Distances (Å) and Angles (deg) for $[L_2Ru_2(\mu\text{-}O)(\mu\text{-}CH_3CO_2)_2](PF_6)_2\cdot 0.5H_2O$

Ru(1)–N(1)	2.112 (4)	Ru(1)–O(3)	2.091 (3)
Ru(1)–N(2)	2.109 (4)	O(2)–C(10)	1.257 (6)
Ru(1)–N(3)	2.168 (4)	O(3)–C(10)	1.255 (6)
Ru(1)–O(1)	1.884 (2)	C(10)–C(11)	1.514 (7)
Ru(1)–O(2)	2.072 (3)	Ru(1)–Ru(1′)	3.258 (1)
N(1)–Ru(1)–N(2)	83.5 (2)	N(1)–Ru(1)–N(3)	82.3 (2)
N(2)–Ru(1)–N(3)	83.0 (2)	N(1)–Ru(1)–O(1)	95.2 (1)
N(2)–Ru(1)–O(1)	95.3 (1)	N(3)–Ru(1)–O(1)	177.1 (2)
N(1)–Ru(1)–O(3)	93.1 (1)	N(2)–Ru(1)–O(3)	168.1 (1)
N(3)–Ru(1)–O(3)	85.3 (1)	O(1)–Ru(1)–O(3)	96.4 (1)
Ru(1)–O(1)–Ru(1′)	119.7 (2)		

two ruthenium(III) ions bridged by an oxo and two acetato groups with two capping tridentate 1,4,7-trimethyl-1,4,7-triazacyclononane ligands. Table V gives atom coordinates, and Table VI summarizes important bond lengths and angles. Each ruthenium(III) center is in a distorted octahedral environment (*fac*-N_3O_3 donor set); the cation possesses crystallographically imposed C_2 symmetry. The Ru–O_{oxo} distance of 1.884 (2) Å is short, indicating considerable double-bond character and resembling in this respect other Ru^{III}–O–Ru^{III} complexes.[35,36] In contrast to the case of the previously characterized (μ-oxo)diruthenium(III) complexes, the Ru–O–Ru unit here is bent (119.7 (2)° vs 157.2 (3) or 165.4 (3)°). The Ru–O_{oxo} bond lengths are not affected; they are very similar.

The Ru–N bond length in the trans position with respect to the Ru–O_{oxo} group is longer by 0.058 Å as compared to the corresponding Ru–N_{cis} distances. This indicates a pronounced trans influence of the μ-oxo bridge. This effect has been observed in complexes $[L_2M_2^{III}(\mu\text{-}O)(\mu\text{-}CH_3CO_2)_2]^{2+}$ characterized by X-ray crystallography (M = V,[11] Fe,[13] Mo[18]). The Ru···Ru distance is 3.258 (1) Å, which is longer by 0.373 Å than the one that has been reported for the only other second-row transition-metal complex of this structural type, namely $[L_2Mo_2^{III}(\mu\text{-}O)(\mu\text{-}CH_3CO_2)_2]^{2+}$,[18] but is *shorter* by 0.182 Å than that in Walton's Os(IV) dimer.[20] For a detailed discussion of the Ru···Ru interaction, see the Discussion. The bond distances of the (μ-oxo)-

Table VII. Atom Coordinates ($\times 10^4$) and Temperature Factors (Å^2 $\times 10^3$) for $[L_2Ru_2(\mu\text{-}O)(\mu\text{-}CH_3CO_2)_2](ClO_4)_2(PF_6)$

atom	x	y	z	U_{eq}[a]
Ru(1)	1108 (1)	1852 (1)	1706 (1)	29 (1)*
Ru(2)	1405 (1)	3146 (1)	571 (1)	34 (1)*
O(1)	1297 (1)	3128 (4)	1337 (2)	33 (2)*
O(2)	624 (1)	1538 (5)	775 (2)	43 (2)*
O(3)	873 (2)	2165 (6)	40 (2)	71 (3)*
C(1)	594 (2)	1729 (7)	188 (3)	37 (3)*
C(2)	184 (2)	1445 (8)	−376 (4)	52 (4)*
O(4)	1473 (2)	542 (5)	1499 (2)	47 (2)*
O(5)	1748 (2)	1531 (5)	883 (3)	61 (3)*
C(3)	1704 (2)	596 (7)	1191 (4)	41 (3)*
C(4)	1947 (3)	−561 (8)	1208 (5)	70 (5)*
N(1)	1531 (2)	1962 (6)	2727 (3)	42 (3)*
N(2)	731 (2)	2922 (6)	2034 (3)	40 (3)*
N(3)	869 (2)	311 (6)	2067 (3)	37 (3)*
C(11)	1357 (2)	2841 (8)	3087 (4)	60 (4)*
C(12)	1029 (2)	3653 (8)	2603 (4)	54 (4)*
C(13)	475 (2)	2071 (7)	2262 (4)	51 (4)*
C(14)	450 (2)	765 (8)	1972 (4)	55 (4)*
C(15)	1139 (2)	101 (8)	2801 (4)	56 (4)*
C(16)	1563 (2)	646 (8)	2972 (4)	51 (4)*
C(17)	1955 (2)	2392 (9)	2814 (4)	61 (4)*
C(18)	457 (3)	3794 (8)	1513 (4)	66 (5)*
C(19)	823 (3)	−866 (7)	1679 (4)	56 (4)*
N(4)	1949 (2)	4221 (6)	932 (3)	46 (3)*
N(5)	1530 (2)	3022 (6)	−316 (3)	52 (3)*
N(6)	1117 (2)	4840 (7)	119 (4)	57 (3)*
C(21)	2189 (3)	3882 (10)	549 (5)	83 (6)*
C(22)	1960 (3)	3525 (11)	−118 (5)	97 (6)*
C(23)	1204 (3)	3783 (12)	−819 (4)	104 (6)*
C(24)	1075 (4)	4877 (9)	−587 (4)	88 (6)*
C(25)	1392 (3)	5783 (8)	547 (5)	108 (6)*
C(26)	1825 (3)	5541 (9)	851 (6)	93 (6)*
C(27)	2216 (3)	4022 (12)	1659 (4)	93 (5)*
C(28)	1502 (5)	1732 (10)	−572 (6)	148 (10)*
C(29)	708 (3)	4944 (14)	93 (7)	145 (9)*
Cl(1)	4252 (1)	6438 (2)	711 (1)	54 (1)*
O(11)	4408 (2)	5454 (6)	1187 (3)	78 (2)
O(12)	3814 (4)	6559 (11)	535 (6)	69 (4)
O(13)	4360 (5)	6368 (14)	166 (7)	82 (4)
O(14)	4439 (4)	7582 (11)	1089 (6)	69 (4)
O(15)	4081 (5)	5908 (16)	35 (8)	112 (6)
O(16)	4576 (5)	7172 (16)	692 (9)	130 (6)
O(17)	3965 (5)	7190 (16)	795 (8)	130 (6)
Cl(2)	1842 (1)	3381 (2)	−2223 (1)	62 (1)*
O(21)	2178 (3)	3408 (10)	−2395 (5)	184 (8)*
O(22)	1840 (3)	2283 (8)	−1902 (5)	154 (6)*
O(23)	1491 (3)	3662 (11)	−2780 (5)	189 (7)*
O(24)	1922 (4)	4339 (10)	−1778 (5)	205 (8)*
P(1)	5000	1647 (3)	2500	57 (2)*
F(11)	4972 (3)	1634 (8)	1794 (4)	188 (6)*
F(12)	4569 (2)	1589 (16)	2332 (5)	305 (10)*
F(13)	5000	2950 (11)	2500	414 (26)*
F(14)	5000	315 (11)	2500	328 (21)*
P(2)	2500	7500	0	53 (1)*
F(21)	2351 (4)	7486 (13)	528 (6)	229 (9)*
F(22)	2835 (4)	8292 (13)	428 (4)	310 (9)*
F(23)	2709 (4)	6325 (12)	344 (7)	297 (11)*

[a] Asterisk indicates equivalent isotropic U_{eq} defined as one-third of the trace of the orthogonalized U_{ij} tensor.

(35) Gilbert, J. A.; Eggleston, D. S.; Murphy, W. R.; Geselowitz, D. A.; Gersten, S. W.; Hodgson, D. J.; Meyer, T. J. *J. Am. Chem. Soc.* **1985**, *107*, 3855.
(36) Phelps, D. W.; Kahn, M.; Hodgson, D. J. *Inorg. Chem.* **1975**, *14*, 2487.

Table VIII. Bond Distances (Å) and Angles (deg) for $[L_2Ru_2(\mu\text{-}O)(\mu\text{-}CH_3CO_2)_2](ClO_4)_2(PF_6)$

Ru(1)–O(1)	1.837 (5)	Ru(1)–O(2)	2.059 (4)
Ru(1)–O(4)	2.070 (6)	Ru(1)–N(1)	2.098 (5)
Ru(1)–N(2)	2.086 (7)	Ru(1)–N(3)	2.137 (7)
Ru(2)–O(1)	1.849 (5)	Ru(2)–O(3)	2.039 (5)
Ru(2)–O(5)	2.051 (5)	Ru(2)–N(4)	2.089 (6)
Ru(2)–N(5)	2.143 (8)	Ru(2)–N(6)	2.105 (7)
C(2)–C(1)	1.246 (9)	O(3)–C(1)	1.244 (11)
C(1)–C(2)	1.487 (8)	O(4)–C(3)	1.248 (11)
O(5)–C(3)	1.245 (10)	C(3)–C(4)	1.494 (12)
Ru(1)–Ru(2)	3.342 (1)		
O(1)–Ru(1)–O(2)	89.9 (2)	O(1)–Ru(1)–O(4)	92.0 (2)
O(2)–Ru(1)–O(4)	90.9 (2)	O(1)–Ru(1)–N(1)	100.9 (2)
O(2)–Ru(1)–N(1)	168.8 (2)	O(4)–Ru(1)–N(1)	100.9 (2)
O(1)–Ru(1)–N(2)	98.1 (2)	O(2)–Ru(1)–N(2)	92.0 (2)
O(4)–Ru(1)–N(2)	169.5 (2)	N(1)–Ru(1)–N(2)	83.5 (2)
O(1)–Ru(1)–N(3)	176.1 (2)	O(2)–Ru(1)–N(3)	86.6 (2)
O(4)–Ru(1)–N(3)	86.3 (2)	N(1)–Ru(1)–N(3)	82.8 (2)
N(2)–Ru(1)–N(3)	83.8 (3)	O(1)–Ru(2)–O(3)	90.9 (2)
O(1)–Ru(2)–O(5)	90.5 (2)	O(3)–Ru(2)–O(5)	92.0 (2)
O(1)–Ru(2)–N(4)	99.7 (2)	O(3)–Ru(2)–N(4)	169.0 (3)
O(5)–Ru(2)–N(4)	90.7 (2)	O(1)–Ru(2)–N(5)	175.9 (2)
O(3)–Ru(2)–N(5)	86.9 (3)	O(5)–Ru(2)–N(5)	86.1 (3)
N(4)–Ru(2)–N(5)	82.7 (3)	O(1)–Ru(2)–N(6)	100.8 (3)
O(3)–Ru(2)–N(6)	91.3 (2)	O(5)–Ru(2)–N(6)	168.2 (3)
N(4)–Ru(2)–N(6)	84.0 (3)	N(5)–Ru(2)–N(6)	82.8 (3)
Ru(1)–O(1)–Ru(2)	130.1 (3)		

Table IX. Formal Redox Potentials for $[L_2Ru_2(\mu\text{-}O)(\mu\text{-}RCO_2)_2](PF_6)_2$ Complexes[a,b]

R	$E_{1/2}$, V vs NHE	E_{red}, V vs NHE	R	$E_{1/2}$, V vs NHE	E_{red}, V vs NHE
CH_3	+0.59 (r)	−1.15 (ir)	C_6H_5	+0.69 (r)	−1.04 (ir)
CF_3	+0.96 (r)	−0.71 (ir)	CCl_3	+0.92 (r)	−0.76 (ir)
H	+0.68 (r)	−1.03 (ir)	CH_2Cl	+0.73 (r)	−0.98 (ir)

[a] Measured in 0.1 M $(TBA)PF_6$ (CH_3CN) at a platinum-button electrode (ferrocene internal standard) at 22 °C at scan rate 100 mV s^{-1}. [b] r = reversible oxidation; ir = irreversible reduction.

bis(μ-acetato)diruthenium(III) core in the present structure and in Sasaki's complex $[(py)_6Ru_2(\mu\text{-}O)(\mu\text{-}CH_3CO_2)_2](PF_6)_2$[28] are identical within experimental error.

The structure of the trication of $[L_2Ru_2(\mu\text{-}O)(\mu\text{-}CH_3CO_2)_2](ClO_4)_2(PF_6)$ is shown in Figure 6; Table VII gives the atom coordinates, and Table VIII summarizes important bond distances and angles. The gross overall structure of the trication is the same as the of the dication discussed in the preceding section. The trication does not possess any crystallographically imposed symmetry. A pronounced trans influence of the μ-oxo group on the $Ru–N_{trans}$ distances is again observed ($d(Ru–N_{trans}) - d(Ru–N_{cis}) = 0.046$ Å). The corresponding Ru–O and Ru–N distances at both ruthenium centers are identical within experimental error.

The most interesting facet of these two structures is the observation that upon removal of one electron from the Ru^{III}_2 dimer all corresponding Ru–O and Ru–N distances *decrease* ($Ru–O_{oxo}$ by 0.041 Å, $Ru–N_{trans}$ by 0.028 Å, $Ru–N_{cis}$ by 0.0165 Å, $Ru–O_{acetato}$ by 0.025 Å); only the Ru···Ru distance *increases* by 0.084 Å. This is in contrast to the simple bonding scheme outlined in the Introduction. Interestingly, in Walton's Os^{IV}_2 dimer the Os···Os distance again increases by 0.098 Å as compared to the Ru···Ru increase in the mixed-valence Ru_2 dimer although the $Os–O_{oxo}$ bond distances are also shorter in the Os^{IV}_2 dimer compared to the corresponding distances in the Ru_2 mixed-valence species (by 0.015 Å).

Electrochemistry. The electrochemistry of the (μ-oxo)bis(μ-carboxylato)diruthenium(III) complexes was studied by cyclic voltammetry and coulometry using platinum electrodes in acetonitrile containing 0.1 M $(PBA)PF_6$ as supporting electrolyte. The half-wave potentials $E_{1/2}$ and E_{red} in V vs NHE at 22 °C are presented in Table IX.

In all cases, one reversible one-electron oxidation at positive potentials and one irreversible reduction peak at negative potentials

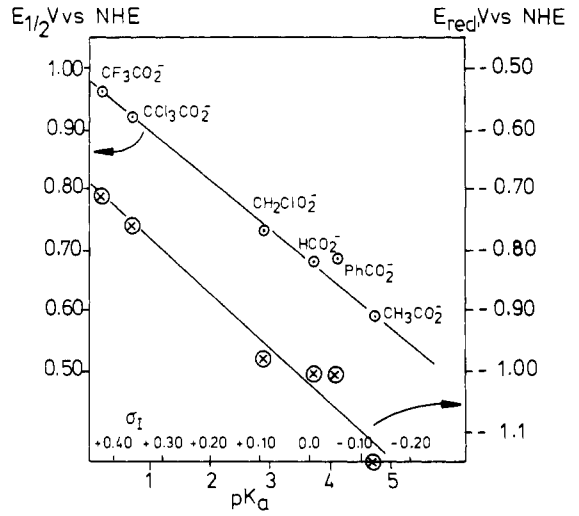

Figure 7. Correlation between the half-wave potentials, $E_{1/2}$ (and the reduction potentials, E_{red}), for $[L_2Ru_2(\mu\text{-}O)(\mu\text{-}RCO_2)_2]^{2+}$ complexes and the pK_a values of the dissociation constant of uncoordinated carboxylic acids.

Scheme II

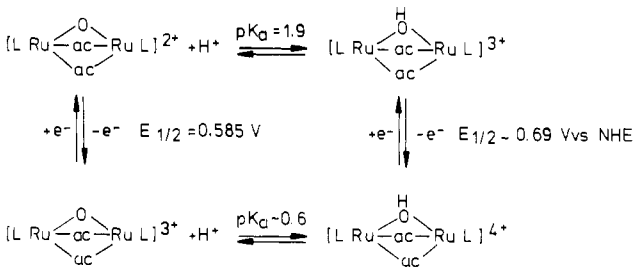

were observed in the potential range +2.0 V to −1.7 V vs Ag/AgCl. For the former, the one-electron transfer per dimer was established by coulometry ($n = 1.0 \pm 0.1$). In the case of the couple between +0.59 and +0.73 V vs NHE, $i_{pa}/i_{pc} \approx 1$, for scan rates (v) between 50 and 200 mV s^{-1}, and the ratio $i_p/v^{1/2}$ was constant, in accord with a diffusion-controlled process. The potential separations, E_p, were in the range 60–85 mV for a scan rate of 100 mV s^{-1}. These observations indicate the reversibility of the one-electron oxidation process. The CV of $[L_2Ru_2(\mu\text{-}O)(\mu\text{-}CH_3CO_2)_2](PF_6)_3$ was identical with that of $[L_2Ru_2(\mu\text{-}O)(\mu\text{-}CH_3CO_2)_2](PF_6)_2$. Very similar electrochemistry has been reported for Walton's (μ-oxo)bis(μ-carboxylato)diosmium complexes.[20]

Interestingly, there appears to exist a fairly linear correlation between $E_{1/2}$ values of the oxidation reaction and the pK_a values of the acid dissociation constant of the uncoordinated carboxylic acids. The same correlation holds for the potentials of the reduction step (Figure 7). A very similar correlation exists using Taft's inductive parameters, σ_I,[33] for the R groups of the carboxylic acids. This is quite reasonable, since the complexes $[L_2Ru_2(\mu\text{-}O)(\mu\text{-}RCO_2)_2]^{2+}$ with electron-withdrawing groups R (CF_3, CCl_3) are the hardest to oxidize, whereas for R = CH_3 (an electron-donating group) oxidation is more readily achieved at less positive potentials. The same arguments apply for the irreversible reduction: electron-withdrawing R groups facilitate the reduction of the ruthenium(III) centers, whereas electron-donating groups render this process more difficult.[37]

The dependence of the redox potential of the reversible oxidation step on the pH of aqueous solutions containing $[L_2Ru_2(\mu\text{-}O)(\mu\text{-}CH_3CO_2)_2](PF_6)_2$ has also been studied at a glassy-carbon electrode at 22 °C. In the range pH 3.5–6 the potential does not

(37) It is noted that a similar dependence of the redox potential of the Co(III)/Co(II) couple on the inductive capacity of $R–CO_2^-$ bridges has been proposed for $[(NH_3)_3Co(\mu\text{-}OH)_2(\mu\text{-}RCO_2)Co(NH_3)]^{3+}$ complexes from kinetic measurements of outer-sphere reductions: Huck, H.-M.; Wieghardt, K. *Inorg. Chem.* **1980**, *19*, 3688.

Table X. Comparison of Structural Parameters[a] for (μ-Hydroxo)bis(μ-carboxylato)dimetal and (μ-Oxo)bis(μ-carboxylato)dimetal Complexes

complex[b]	M···M, Å	M–$O_{oxo/hydroxo}$, Å	M–N_{trans}, Å[c]	M–N_{cis}, Å[d]	M–$O_{acetate}$, Å	M–O–M, deg	ref
1	3.120	1.800	2.268	2.198	2.034	119.7	2, 13
2	3.439	1.956	2.102	2.102	1.994	123.1	3
3	3.555	2.090	2.197	2.196	2.087	115.4	18
4	2.885	1.945	2.294	2.253	2.096	95.7	18
5	2.969	1.920	2.256	2.208	2.048	101.3	18
6	3.258	1.884	2.168	2.110	2.080	119.7	this work, 19
7	3.342	1.843	2.140	2.094	2.055	130.1	this work, 19
8	3.440	1.830			2.111	140.2	20
9	3.251	1.857	2.208	2.08	2.086	122.2	28
10	3.290	1.794	2.228	2.158	2.048	130.2	11

[a] Bond distances are average values (except M···M distances). [b] Key: **1**, $[L_2Fe_2(\mu\text{-}O)(\mu\text{-}CH_3CO_2)_2](ClO_4)_2\cdot H_2O$; **2**, $[(HB(pz)_3)_2Fe_2(\mu\text{-}OH)(\mu\text{-}CH_3CO_2)_2](ClO_4)\cdot 0.5CH_2Cl_2$; **3**, $[L_2Mo_2(\mu\text{-}OH)(\mu\text{-}CH_3CO_2)_2](ClO_4)_3\cdot H_2O$; **4**, $[L_2Mo_2(\mu\text{-}O)(\mu\text{-}CH_3CO_2)_2](ClO_4)(BF_4)\cdot H_2O$; **5**, $[L_2Mo_2(\mu\text{-}O)(\mu\text{-}CH_3CO_2)_2](ClO_4)_3\cdot H_2O$; **6**, $[L_2Ru_2(\mu\text{-}O)(\mu\text{-}CH_3CO_2)_2](PF_6)_2\cdot 0.5H_2O$; **7**, $[L_2Ru_2(\mu\text{-}O)(\mu\text{-}CH_3CO_2)_2](ClO_4)_2(PF_6)$; **8**, $[Os_2(\mu\text{-}O)(\mu\text{-}CH_3CO_2)_2Cl_4(PPh_3)_2]\cdot(C_2H_5)_2O$; **9**, $[Ru_2(\mu\text{-}O)(\mu\text{-}CH_3CO_2)_2(py)_6](PF_6)_2$; **10**, $[L_2V_2(\mu\text{-}O)(\mu\text{-}CH_3CO_2)_2]I_2\cdot 2H_2O$. [c] M–N distance trans to the M–$O_{oxo/hydroxo}$ bond. [d] M–N distance cis to the M–$O_{oxo/hydroxo}$ bond.

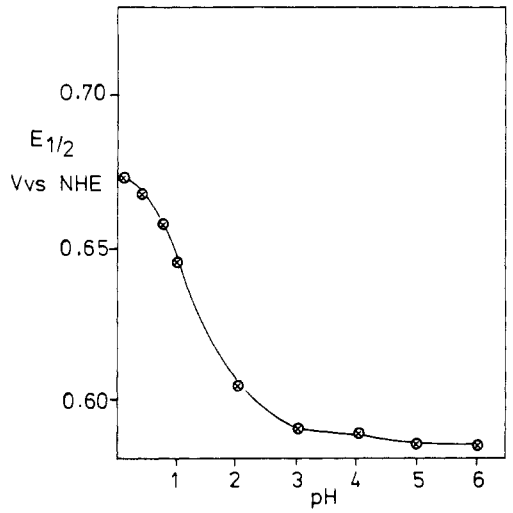

Figure 8. pH dependence of the redox potential, $E_{1/2}$, of the reversible oxidation of $[L_2Ru_2(\mu\text{-}O)(\mu\text{-}CH_3CO_2)](PF_6)_2$ in aqueous buffer solutions at a glassy-carbon electrode at 22 °C.

change (+0.585 V vs NHE). This value corresponds nicely to the one obtained in acetonitrile (Table IX). With decreasing pH (3–0), the potential increases to 0.675 V vs NHE. The near sigmoidal shape of the curve in Figure 8 is compatible with Scheme II, where the μ-hydroxo-bridged dimer is reversibly oxidized ($E_{1/2} \approx 0.68$ V vs NHE) to yield the mixed-valence μ-OH-bridged dimer. At higher pH values the μ-oxo-bridged dimer is reversibly oxidized. Two pK_a values of 1.9 and ≈0.6 may be calculated from Figure 8, which correspond to the protonation–deprotonation reaction of the $Ru(III)_2$ dimer and of the mixed-valence dimer, respectively.

Discussion

The question we wish to address first concerns the nature of the Ru···Ru interaction in the (μ-oxo)bis(μ-acetato)diruthenium(III) core and in its mixed-valence form, the (μ-oxo)bis(μ-acetato)diruthenium(III/IV) complex. Two distinctly different models can be envisaged: (i) The metal–metal distance is primarily dictated by the geometry of the bridging groups (Ru–O_{oxo} distances and the Ru^{III}–O–Ru^{III} bond angle) or (ii) direct metal–metal bonding is at least a contributing factor to the observed metal–metal distance.

Complexes containing the (μ-oxo)bis(μ-carboxylato)dimetal core may be viewed as cofacial bioctahedral species where the ideal D_{3h} symmetry of a molecule with three identical μ-X bridging groups is lowered to effective C_{2v} by substituting two of these by two symmetrically bridging carboxylato bridges. If the Ru–O_{oxo} vectors are taken as z axes, the t_{2g} atom orbitals of the ruthenium centers may be used to construct symmetry-allowed Ru···Ru molecular orbitals. On the basis of the analyses of McCarley et al.,[38] Hoffmann et al.,[39] Wentworth et al.,[40] and Cotton et al.,[41] one σ-bonding and two—in C_{2v} nondegenerate—π-bonding MO's and one σ^*- and two π^*-antibonding MO's are obtained, which are primarily involved in direct metal–metal bonding. For the (μ-oxo)bis(μ-carboxylato)diruthenium(III) complexes an electron distribution ($\sigma^2\pi^4\pi^{*4}$) and a Ru–Ru bond of the order 1 would follow from this simple model and, in addition, a singlet ground state of the molecule is predicted—in agreement with the observed diamagnetism.

Oxidation of the diruthenium(III) complexes by one electron per dimer would yield a mixed-valence species with a $\sigma^2\pi^4\pi^{*3}$ configuration and a Ru–Ru bond of the order 1.5. Thus, this model predicts a decrease of the Ru–Ru distance on going from the $Ru(III)_2$ dimer to its oxidized form—in contrast to the observation—and a doublet ground state for the $Ru^{III}Ru^{IV}$ species, which is observed. It should be noted that there is one well-documented example in the literature where a similar discrepancy between the theoretical expectations and observed metal–metal bond distances appears to exist. The Tc–Tc distance in $[Tc_2Cl_8]^{3-}$ ($\sigma^2\pi^4\delta^2\delta^{*1}$) is *shorter* by 0.030 Å than that in its oxidized form $[Tc_2Cl_8]^{2-}$ ($\sigma_2\pi_4\delta_2$), despite the fact that in the reduced form an antibonding metal–metal MO is occupied.[42] On the other hand, the model correctly accounts for the observed Mo–Mo distances in the complexes $[L_2Mo^{III}_2(\mu\text{-}O)(\mu\text{-}CH_3CO_2)_2]^{2+}$ and $[L_2Mo^{III}Mo^{IV}(\mu\text{-}O)(\mu\text{-}CH_3CO_2)_2]^{3+}$.[18] In the former a short Mo–Mo bond (2.885 (1) Å) of the order 3 ($\sigma^2\pi^4$) has been established, and in the oxidized form a slightly longer Mo–Mo bond of the order 2.5 ($\sigma^2\pi^3$) has been found. The Os(IV)–Os(IV) distance in Walton's diamagnetic dimer is 3.440 Å, which together with the present data on the Ru^{III}_2 dimer and the $Ru^{III}Ru^{IV}$ species certainly rules out an Os–Os bond of the order 2, as would be expected in the frame of the above model ($\sigma^2\pi^4\pi^{*2}$).

A closer comparison of the structural data for the Ru^{III}_2, $Ru^{III}Ru^{IV}$, and Os^{IV}_2 dimers with those for other (μ-oxo)bis(μ-acetato)dimetal cores as summarized in Table X is instructive. To a first approximation, the effective ionic radii of ruthenium and osmium centers in a given oxidation state within a dimer (III,III; III,IV; IV,IV) are identical.[43] It is then reasonable and is observed that the metal–oxo bond distances *decrease* upon stepwise oxidation of the dimetal(III) species to the dimetal(IV) complex; but at the same time the metal–metal distance is observed to *increase*. This is somewhat counterintuitive and may be an indication of an increasing electrostatic repulsion between the metal ions upon oxidation, which forces the metal ions further apart. This repulsion must override possible attractive bonding interactions between these centers, and the observed distances are

(38) Templeton, J. L.; Dorman, W. C.; Clardy, J. C.; McCarley, R. E. *Inorg. Chem.* **1978**, *17*, 1263.
(39) Summerville, R. H.; Hoffmann, R. *J. Am. Chem. Soc.* **1979**, *101*, 3821.
(40) Scillant, R.; Wentworth, R. A. D. *J. Am. Chem. Soc.* **1969**, *91*, 2174.
(41) Cotton, F. A.; Ucko, D. A. *Inorg. Chim. Acta* **1972**, *6*, 161.
(42) Cotton, F. A.; Daniels, L.; Davison, A.; Orvig, C. *Inorg. Chem.* **1981**, *20*, 3051.
(43) (a) Shannon, R. D.; Prewitt, C. T. *Acta Crystallogr., Sect. B* **1969**, *B25*, 925. (b) Shannon, R. D. *Acta Crystallogr., Sect. A* **1976**, *A32*, 751.

a compromise between two opposingly acting repelling and attractive forces.

It is also instructive to compare the structural data for the (μ-oxo)bis(μ-acetato)diiron(III) complex and its vanadium(III) analogue with those for the diruthenium(III) species. The diiron(III) complex consists of two high-spin iron(III) centers that are strongly antiferromagnetically coupled ($J = -119$ cm^{-1}); the effective ionic radius of octahedral high-spin iron(III) is 0.785 Å. The vanadium(III) analogue exhibits weak ferromagnetic coupling of the d^2–d^2-configured centers, and the effective ionic radius is also 0.78 Å. In both complexes the observed magnetism rules out appreciable metal–metal bonding; the M···M distances are 3.120 and 3.250 Å, respectively. The effective ionic radius of low-spin ruthenium(III) in an octahedral environment is 0.82 Å, which is very similar to those of high-spin Fe(III) and V(III), and the observed Ru···Ru distance of 3.258 Å in $[L_2Ru_2(\mu\text{-}O)(\mu\text{-}CH_3CO_2)_2]$ also agrees very well with those found in the iron(III) and vanadium(III) dimers. Therefore, we conclude that the existence of a Ru–Ru bond cannot be deduced from the structural data at hand.

The diamagnetism of the Ru^{III}_2 complexes is then interpreted by using a delocalized description for the Ru–O–Ru moiety as has been described by Meyer et al.[34] (for oxo-bridged ruthenium(III) dimers containing a nearly linear Ru–O–Ru arrangement) and, in addition, by using a through-space Ru···Ru interaction of the type described above. The delocalized MO description is a favorable one, since the mixed-valence species is formed at reasonable potentials (an electron is removed from a π^* level and is not a metal-centered Ru(III) to Ru(IV) oxidation) and the intense, low-energy bands in the visible spectra can be assigned to $\pi^b \rightarrow \pi^*$ transitions involving delocalized Ru–O–Ru levels.

Protonation of the μ-oxo bridge in (μ-oxo)bis(μ-carboxylato)diruthenium(III) complexes effects a dramatic change in the electronic and magnetic properties. Although we have not been able to grow single crystals suitable for X-ray crystallography of such a (μ-hydroxo)bis(μ-carboxylato)diruthenium(III) species, we propose that protonation leads to a significantly longer Ru^{III}–$O_{hydroxo}$ bond as compared to the Ru–O_{oxo} bonds in the analogous oxo complexes.[47] As a consequence of this, the two ruthenium(III) centers are further apart. Interestingly, the structure of a μ-aqua-bridged ruthenium(II) dimer has been reported, namely (μ-aqua)bis(μ-trifluoroacetato)bis[(η^4-cycloocta-1,5-diene)(trifluoroacetato)ruthenium(II)], where the Ru–OH_2 bond distance is 2.164 (5) Å and the Ru···Ru distance is 3.733 (1) Å.[44] We have recently reported a diamagnetic (μ-acetato)bis(μ-hydroxo)bis[(1,4,7-triazacyclononane)ruthenium(III)] triiodide,[45] where the Ru–$O_{hydroxo}$ distance is 2.024 Å and the Ru^{III}–Ru^{III} distance is 2.572 Å. Since the Ru–$O_{acetato}$ distances (2.067 Å) of this complex are quite similar to those found here for the (μ-oxo)bis(μ-acetato)diruthenium(III) complex (2.080 Å), we feel that a Ru^{III}–$O_{hydroxo}$ distance of 2.024 Å may also prevail in the (μ-hydroxo)bis(μ-acetato)diruthenium(III) complex, which would be longer by 0.14 Å than the Ru^{III}–O_{oxo} bond distance. In two instances, both the protonated μ-hydroxo- and μ-oxo-bridged complexes have been characterized by X-ray crystallography. These studies involve the central ions molybdenum(III)[18] and iron(III);[2,3,13] for the former the difference in M–O bond lengths is 0.145 Å, and for the latter system 0.156 Å has been determined. In both systems the M–$O_{acetato}$ bonds differ maximally by 0.040 Å (Table X).

This protonation perturbs the delocalized Ru–O–Ru moiety and the direct Ru···Ru interaction to such an extent that at room temperature the (μ-hydroxo)bis(μ-carboxylato)diruthenium(III) center is paramagnetic.

The mixed-valence complex $[L_2Ru_2(\mu\text{-}O)(\mu\text{-}CH_3CO_2)_2](ClO_4)_2(PF_6)$ appears to be the first structurally characterized $Ru^{III}Ru^{IV}$ dimer. Meyer et al. have recently described two μ-oxo-bridged dimers $[(bpy)_2(OH_2)Ru^{III}ORu^{IV}(OH)(bpy)_2](ClO_4)_4$[35] and $[(bpy)_2ClRu^{III}ORu^{IV}Cl(bpy)_2](PF_6)_3$.[34] For the latter species the equivalence of the two ruthenium centers was deduced from an ESCA study,[34] and the compound has been described as an example of a class III case in the Robin and Day mixed-valence classification scheme.[46] In the present case this assignment is corroborated by the observation of a band in the near-IR region at 1591 nm ($\epsilon = 276$). In addition, in the solid state both Ru centers are equivalent within experimental error.

Acknowledgment. We are grateful to the Fonds der Chemischen Industrie for financial support of this work and to Degussa (Hanau, FRG) for a generous gift of $RuCl_3 \cdot nH_2O$. We thank Professors Y. Sasaki (Sendai, Japan) and T. J. Meyer (Chapel Hill, NC) for communicating their results prior to publication. T. J. Meyer is also thanked for helpful discussions.

Registry No. **6**, 115140-51-7; **7**, 115140-45-9; $[LRuCl_3]\cdot H_2O$, 118018-83-0; $RuCl_2(dmso)_4$, 59091-96-2; $[L_2Ru_2O(CH_3CO_2)_2](PF_6)_2$, 115140-44-8; $[L_2Ru_2O(HCOO)_2](PF_6)_2$, 118018-85-2; $[L_2Ru_2O(CF_3CO_2)_2](PF_6)_2$, 118041-47-7; $[L_2Ru_2O(C_6H_5CO_2)_2](PF_6)_2$, 118018-87-4; $[L_2Ru_2O(CCl_3CO_2)_2](PF_6)_2$, 118018-89-6; $[L_2Ru_2O(CH_2ClCO_2)_2](PF_6)_2$, 118018-91-0; $[L_2Ru_2(OH)(CH_3CO_2)_2](PF_6)_3$, 115140-47-1; $Na_2S_2O_8$, 7775-27-1; $[L_2Ru_2(\mu\text{-}O)(\mu\text{-}CH_2)_2](PF_6)_3$, 115140-49-3; D_2, 7782-39-0; $[L_2Ru_2(\mu\text{-}OH)(\mu\text{-}CH_3CO_2)_2](ClO_4)_3$, 118018-92-1.

Supplementary Material Available: Tables S1–S9, listing additional crystallographic data, anisotropic thermal parameters, hydrogen coordinates and isotropic thermal parameters, and bond angles and distances for $[L_2Ru_2(\mu\text{-}O)(\mu\text{-}CH_3CO_2)_2](PF_6)_2\cdot 0.5H_2O$ and $[L_2Ru_2(\mu\text{-}O)(\mu\text{-}CH_3CO_2)_2](ClO_4)_2(PF_6)$ (9 pages); Tables S10 and S11, listing observed and calculated structure factors for both compounds (48 pages). Ordering information is given on any current masthead page.

(44) Albers, M. O.; Liles, D. C.; Singleton, E.; Yates, J. E. *J. Organomet. Chem.* **1984**, *272*, C62.
(45) Wieghardt, K.; Herrmann, W.; Köppen, M.; Jibril, I.; Huttner, G. *Z. Naturforsch.* **1984**, *39B*, 1335.
(46) Robin, M. B.; Day, P. *Adv. Inorg. Chem. Radiochem.* **1967**, *10*, 247.
(47) After this paper had been accepted for publication, we were able to solve the crystal structure of $[L_2Ru_2(\mu\text{-}OH)(\mu\text{-}CH_3CO_2)_2](ClO_4)_3$. The Ru–$O_{hydroxo}$ bond distance was found to be 1.98 (2) Å, and the Ru···Ru distance, 3.472 (2) Å. Details of this crystal structure determination will be published elsewhere.